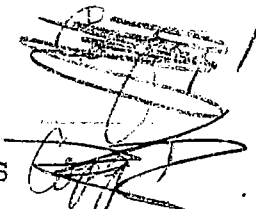


34  
Library L. M. A. L.  
AUG 7 1937  
1102.21  
-45  


TECHNICAL MEMORANDUMS

NATIONAL ADVISORY COMMITTEE FOR AERONAUTICS



3 1176 00090 5787

No. 834

THE STABILITY OF ORTHOTROPIC ELLIPTIC CYLINDERS  
IN PURE BENDING

By O. S. Heck

Luftfahrtforschung  
Vol. 14, No. 3, March 20, 1937  
Verlag von R. Oldenbourg, Munchen und Berlin

FILE COPY

To be returned to  
the files of the Langley  
Memorial Aeronautical  
Laboratory

Washington  
July 1937

NATIONAL ADVISORY COMMITTEE FOR AERONAUTICS

TECHNICAL MEMORANDUM NO. 834

THE STABILITY OF ORTHOTROPIC ELLIPTIC CYLINDERS  
IN PURE BENDING\*

By O. S. Heck

The theoretical critical bending stress of elliptic cylindrical shells is determined on the assumption of infinite shell length and absence of local instability phenomena. The results of tests on isotropic elliptic cylindrical shells stressed in bending are compared with the theoretical results. The practical applicability of the theory is discussed.

I. INTRODUCTION

The preliminary calculation of the load capacity of a thin-walled cylindrical shell under bending stress is of importance in airplane statics in the analysis of shell bodies. Hereby it does not merely pertain to isotropic circular cylindrical shells which, in the literature up to now, are almost exclusively used in bending tests, but also, above all, to the bending of orthotropic (orthogonally anisotropic\*\* and stiffened cylindrical shells. The study of shells with other than circular sections (elliptic, for example) is of particular practical importance.

General application of Navier's simple bending theory to thin-walled beams is no longer permissible, according to Prandtl, because of the occasionally enormous strain of the section under load. On the strength of this, and prompted by experiments on elastic balance tubes, von Kármán investigated the bending of curved thin-walled pipes (reference 1). But his findings are inapplicable to straight pipes. Besides, von Kármán failed to mention the important fact that the bending moment has a maximum (crit-

---

\*"Über die Stabilität orthotroper elliptischer Zylinderschalen bei reiner Biegung." Luftfahrtforschung, vol. 14, no. 3, March 20, 1937, pp. 137-147.

\*\*The concept of orthogonally anisotropic plate was probably first given by M. T. Huber (cf. Bauing., vol. 4, 1923, p. 354.

ical) value conditioned by the flattening of the cross section.

The first study on the pure bending of infinitely long isotropic circular cylindrical shells, was made by Brazier (reference 2). He shows that the bending moment does not increase linearly with the curvature of the shell axis and that it assumes a maximum (critical) value for a certain curvature of the shell axis; for greater curvature the system ceases to be stable.

This type of instability (similar instability prevails under compression and bending of a bar) is essentially different from that encountered in the usual stability problems, such as in the buckling of a straight bar, for example.

Figure 1 shows the behavior of a straight compression member. The load  $P$  runs linear to the approach of the bar ends as far as the branching-off point (buckling load). From that point on, there are two possible conditions of equilibrium: the bar may remain straight - that is, in unstable equilibrium, or deflect sideways under stable equilibrium. In both cases the load  $P$  increases beyond the buckling load.

Brazier's discussion of bending of a cylindrical shell is illustrated in figure 2. The curve which gives the bending moment  $B$  relative to the curvature  $\kappa$  of the shell axis, has no branching-off point. The bending moment cannot be increased beyond the critical value  $B_{kr}$ . After the critical condition is exceeded there remains only one possible equilibrium condition of the shell, and that is: unstable.

Figure 3 finally shows the behavior of a cylindrical shell in bending when accompanied by local buckles which belong to the instability phenomena of the usual type. The maximum load supported by the shell is more or less reduced by the buckles; hence Brazier's value obtained by disregarding a local buckling, constitutes a theoretical upper limit of the maximum load in an infinitely long shell.

## II. FORMULATION OF PROBLEMS AND ASSUMPTIONS

In the present report the behavior of orthotropic

cylindrical shells of elliptic section in pure bending is theoretically investigated. Critical bending moment, critical bending stress, and deformation of shell section are determined. The principal assumptions are as follows:

1. The cylindrical shell is of infinite length,
2. There are no local instability phenomena (i.e., no wrinkling).
3. The stresses remain below the proportional limit of the material.

The value of our findings for practical application, if premises 1 and 2 are not met, is discussed in the next section. Whether assumption 3 is fulfilled can always be verified.

The local instability of long shells can be investigated when allowance for the strain condition - i.e., the change in curvature radius of the shell section and of the distances from the zero line - is made in accordance with the considerations of the present report. An approximate study of local instability has been made by Brazier for the case of isotropic circular cylindrical shell. But the local instability is so seriously affected by inevitable preliminary wrinkling that theoretical studies which do not allow for these preliminary wrinkles, are of limited practical importance only.

### III. RESULTS AND SCOPE OF VALIDITY

The critical bending moment  $B_{kr}$  of an orthotropic cylindrical shell of elliptic section stressed in bending in the major or minor axis of the section is on the assumptions cited in the preceding section:

$$B_{kr} = W \sigma_{kr} \quad (1)$$

with

$$\sigma_{kr} = c \frac{E}{\sqrt{1 - \nu^2}} \frac{s}{\rho} \sqrt{\frac{s}{s_m}} \quad (2)$$

Hereby

- E is the modulus of elasticity of the material
- $\nu$ , Poisson's ratio (about 0.3 for steel and duralumin)
- s, wall thickness of shell
- $s_m$ , mean wall thickness, which governs the stiffness of the shell to axial stresses (in the case of the shell with closely spaced stringers, which approximately resembles an orthotropic shell, it is:  $s_m = s + \frac{F}{u}$ , where  $F$  = total section of stringers, and  $u$  = circumference of section of mean shell surface)\*
- a, b, major and minor half axis of the shell section
- $\rho$ , radius of curvature of undeformed shell section at the point of stress peak ( $\rho_g = a^2/b$  under bending on the major sectional axis  $\rho_k = b^2/a$  by bending on the minor sectional axis)
- W, section modulus of undeformed cross section of the elliptic cylinder
- $$(W_g = \frac{\pi}{4} b (b + 3a) s_m)$$
- referred to major sectional axis
- $$W_k = \frac{\pi}{4} a (a + 3b) s_m$$
- referred to minor sectional axis)
- $\sigma_{kr}$ , critical bending stress ( $\sigma_{kr}$  is simply a fictitious stress, because W refers to the undeformed cross section of the shell)
- c, a numerical value which depends on axes ratio  $a/b$  of the shell section or the value  $k^2 = \frac{a^2 - b^2}{a^2}$  and may be obtained from figure 4.

The subscripts g and k indicate, respectively, the bending about the major and minor cross-sectional axes.

---

\*Uniform stringer distribution being assumed.

For a shell having unlike moduli of elasticity in longitudinal and circumferential directions, the critical bending stress is:

$$\sigma_{kr} = c \sqrt{\frac{E_1 E_2}{1 - \nu^2}} \frac{s}{\rho} \quad (3)$$

where  $E_1$  = modulus of elasticity in circumferential, and  $E_2$  in longitudinal, direction of the shell.

The "real" critical bending stress  $\sigma_{kr}'$  (in contradistinction to the "fictitious" critical stress  $\sigma_{kr}$ ) must not - if the findings of this study are to retain their validity - exceed the proportional limit of the material. To decide whether this condition is fulfilled, compute  $\sigma_{kr}'$  according to (2) or (3) whereby  $c_g'$  and  $c_k'$  obtainable from figure 5, replace  $c_g$  and  $c_k$ .

The extent of the cross-sectional strain may be seen from figures 6 and 7, where the relative length changes in the axes of the shell section, on reaching the critical condition, are plotted.\*

In the calculation of the quantities plotted in figures 4 to 7, the squares and products of the displacement components of the shell element in their cross-sectional plane were disregarded relative to the first powers of these values, as in Brazier's study. To gain an idea of the effect of this omission, we made a more accurate calculation for  $k^2 = 0$  and  $k^2 = 0.3$ , the results of which are also included in figures 4 to 7. But even these values are not absolutely correct, since there are still other influences which are not considered in the calculation. In the calculation of the curvature change of the shell section, for example, the displacement components of the shell elements in the cross-sectional plane are considered as small; i.e., higher powers of these values are neglected relative to the first powers. Further, it was assumed that the strain in the shell section consists solely in a deflection, but not in a length change of the line elements of the shell section. The more exact calculation gives greater values for  $\sigma_{kr}$ , so that the appli-

---

\*w is the shifting of a cross-sectional point at right angles to the circumference (positive inward). The explanation for  $w_0$  and  $w\pi/2$  will be found in figures 12 and 13.

cation of the results of the simple calculation leaves one on the safe side. Experimental verification of the theory seems, in the face of these facts, absolutely necessary.

In the following, the extent of the practical application of equations (1) to (3) to cases where assumptions (1) and (2) are fulfilled, is discussed.

a) Isotropic shells.— In isotropic shells, even if of great length, the beginning of the instability through collapse of the shell walls toward the neutral axis, is initiated by a local wrinkling on the compression half of the cylinder, as a result of which the failing load of the shell is reduced. Numerous experiments on isotropic circular, cylindrical shells (cf. figs. 17 to 19) have shown that the average maximum bending moment supported by the shells is not very much different from the theoretical value for the infinitely long shell without consideration to local instability phenomena.

The average value of  $c$  of 77 tests is  $c_{\text{average}} = 0.357$ . But the scatter of the experimental values is in part quite considerable. From the available test data there is no indication of any effect of shell length (fig. 19).

For the purpose of checking the applicability of the theoretical values arrived at with the assumptions outlined in section II, for elliptic cylindrical shells of finite length, we made several experiments with isotropic elliptic cylindrical shells of varying axes ratios. The tests disclose through the theoretical values computed with the coefficients  $c_g$  and  $c_k$  a good agreement for bending about the major cross-sectional axis, but markedly lower experimental values for bending about the minor cross-sectional axis. (Cf. section IV and fig. 4.)

In the latter case, it means that local wrinkling of the shell wall results in a material reduction of failing load of the shell, contrary to the experiences with circular cylindrical and elliptic cylindrical shells in bending about the major cross-sectional axis. A certain explanation for this fact may be found when assuming that the failure then occurs in the event that the axial stress  $\sigma$  in the shell reaches at some point of the cross section the critical value  $\sigma_{kr}$  of equation (2). This most un-

favorably stressed point follows from the condition that the product of curvature radius of shell section and the distance from the neutral zone must become a maximum. When disregarding the strain of the shell section this point is given by

$$t = \arcsin \frac{1}{2k} \quad (k^2 > 0.25)$$

Then the critical bending moment can be computed from the formulas (1), (2), and (3), is at  $k^2 > 0.25$  instead of  $c_k$  the coefficient

$$\bar{c}_k = \frac{16}{3\sqrt{3}} k (1 - k^2)^{3/2} c_k$$

is substituted. At  $k^2 \leq 0.25$  the extreme fiber on the compression half of the shell is most adversely stressed. Figure 4 shows  $\bar{c}_k$  plotted against  $k^2$ . The agreement with the experimental values is comparatively good.

b) Orthotropic shells.— While the local bulging of the walls of a shell with lengthwise closely spaced stiffeners, which approximately resembles an orthotropic shell, is dependent on the bending stiffness of these stiffeners, the failure due to collapse of the shell walls is dependent on its cross section. There is no local bulging of shell walls before failure in very long elliptic shells with closely spaced stringers for sufficiently high bending stiffness and small cross section. In that case the results of the present report are exactly valid.

As concerns the applicability of the theoretical formula and the effect of shell length in orthotropic elliptic shells (plywood shells, for instance), no experiments are available. For computing the failing moment of short stiffened shells with strong fairly closely spaced frames, the results of this study are inapplicable as the restrained flattening of the shell section increases the failing load of such shells as a rule very considerably compared to the failing load of very long shells without frames.\* If the strain of the section of such a shell is

---

\*The theoretical formula (2) is also useful for calculating the closed part of a shell body with comparatively closely spaced intermediate bulkheads, since it indicates the critical bending stresses for the collapse of the shell walls in buckling form; that is, a lower limit in shells of  
(Continued at bottom of page 8)



negligibly small, then the study of the local stability of the assumedly orthotropic shell is comparatively simple as against the general case, because the bending moment up to stability limit runs linear with the curvature of the shell axis. As regards the bulging of the walls of orthotropic shells, a better agreement between theory and test seems indicated than with isotropic shells, since the inevitable preliminary bulges are smaller in comparison with the mean wall thickness.

#### IV. EXPERIMENTS WITH ISOTROPIC ELLIPTIC CYLINDERS

A series of failing tests in pure bending about the major and minor cross-sectional axes was carried out on isotropic elliptic cylindrical shells of duralumin of two different axes' ratios. The dimensions of the test specimens are given in table I. ( $l$  is the free length of the cylindrical shell.) The modulus of elasticity of the material was established at  $E = 7.5 \times 10^5 \text{ kgcm}^{-2}$ . The evaluation of the tests was made with  $\nu = 0.3$  Poisson's ratio. The experimental arrangement itself is illustrated in figure 8. The wooden frames at the ends of the test cylinder serve to press the sheet against them through exactly fitting wooden jigs. One end frame is clamped to a solid frame while a pure bending moment is applied at the other frame. The weight of this frame is compensated. Two failing tests could be made on each specimen. After the first test the cylinder was turned through  $180^\circ$  on its axis, which left the still undamaged part of the specimen on the compression half of the cylinder for the second test.

TABLE I. Dimensions of Test Specimens

Specimen	a	b	l	s
	cm	cm	cm	cm
1	22.5	15	78	0.050
2	30	15	127	.051

\*(Continued from footnote, page 7)  
of finite length, which are bounded by fixed ribs. Logically, the thickness of a smooth sheet must thereby be written for  $s$  in (2), whose bending stiffness equals the mean bending stiffness of the stiffened shell in circumferential direction under consideration of the frames. One obtains in this manner a control point for the rib dimensions.

The results of the failing tests are given in table II. For comparison with the theoretical values (admittedly derived for infinitely long cylindrical shell and disregarded local instability phenomena), we have included the experimental values of  $c_g$  and  $c_k$  in figure 4. A discussion of the test data is given in the preceding section.

TABLE II. Test Data

Specimen	Bending about major cross-sectional axis					Bending about minor cross-sectional axis				
	$\rho_g$	$W_g$	$B_{g_{kr}}$	$\sigma_{g_{kr}}$	$c_g$	$\rho_k$	$W_k$	$B_{k_{kr}}$	$\sigma_{k_{kr}}$	$c_k$
	cm	cm <sup>3</sup>	cmkg	kgcm <sup>-2</sup>	-	cm	cm <sup>3</sup>	cmkg	kgcm <sup>-2</sup>	-
1	33.75	48.5	19600	405	.347	10	59.6	42500	713	.181
			21200	437	.375			47300	794	.202
2	60	63.1	17350	275	.411	7.5	90.1	53700	595	.111
			16900	268	.401			52200	580	.108

## V. THEORETICAL ANALYSIS

### 1. Formulation of Problem as Variation Problem

To analyze the behavior of a circular or elliptic cylindrical shell in pure bending, we resort to the principle of minimum potential energy. The assumption of infinite shell length neutralizes eventual edge effects. Conformable to another assumption, there is to be no local bulging of shell walls. Then all sections of the shell are strained in the same fashion for reasons of symmetry, so that the analysis can be restricted to a piece of shell of length  $l$ .

For a given curvature  $\kappa$  of the shell axis, the form which the shell section assumes must be so defined that by fixed  $\kappa$  the energy of form change  $U$  becomes a minimum. So if the strain of the shell section and consequently, the energy of form change  $U$  is known in relation to curvature  $\kappa$ , the bending moment  $B$  follows as derivative of  $U$  with respect to  $\kappa$ .

The form change energy  $U$  comprises:

- 1) The form change energy  $U_1$ , corresponding to the strain of the shell section.
- 2) The form change energy  $U_2$ , corresponding to the length changes of the shell fibers.

The strain of the shell section is assumed to consist only in a deflection but not in a length change of the linear elements of the section of the middle of the shell. It is assumed that both strains corresponding to the energy of form changes  $U_1$  and  $U_2$  take place successively, for example -- first the strain of the shell section and then the elongations or contractions in shell-length direction. The additional strain of the shell section following the initiation of the axial stresses as a result of transverse contraction, is small enough to be negligible.

It is then:

$$U_1 = \frac{E}{2} \frac{s^3}{12 (1 - \nu^2)} J_1 \quad (4)$$

$$U_2 = \frac{E}{2} s_m \kappa^2 J_2 \quad (5)$$

with

$$J_1 = \oint (\Delta \kappa_u)^2 du \quad (6)$$

$$J_2 = \oint h^2 du \quad (7)$$

whereby the integrals extend over the whole circumference of the shell section. It is:

$\kappa$ , curvature of the shell axis

$\Delta \kappa_u$ , change in curvature of the section of the median shell area

$u$ , arc length of the section of the median shell area

$h$ , distance of an element of the strained shell from the neutral axis

Assume the strain of the shell section to be defined by the natural coordinates  $v$  and  $w$  of the displacement of the shell elements in the sectional plane:  $v$ , to denote the component of displacement in tangential direction (pos-

itive in the sense of increasing  $u$ ) and  $w$ , the component in normal direction (the inside normal to be positive) of the undeformed section. The curvature change  $\Delta \kappa_u$  of the shell section, which may be any, so long as it has no corners, can be expressed with Frenet's formulas through the displacement components  $v$ ,  $w$ , and their derivatives. We have:

$$\Delta \kappa_u = \frac{w}{\rho^2} + w'' - v \frac{\rho'}{\rho^2} \quad (8)$$

Here  $\rho$  is the radius of curvature of the shell section (positive if the center of curvature lies on the inside normal),  $\rho'$  the first derivative of  $\rho$  with respect to arc length  $u$ , and  $w''$  the second derivative of  $w$  with respect to  $u$ . If, as according to our premise, the length of the linear elements of the section is constant, then there exists between  $v$  and  $w$ , the relation:

$$w = \rho v' \quad (9)$$

With due regard to (9), equation (8) becomes:

$$\Delta \kappa_u = \rho v''' + 2\rho' v'' + \left(\rho'' + \frac{1}{\rho}\right) v' - v \frac{\rho'}{\rho^2} \quad (10)$$

It will be observed that in (8) to (10) the higher powers of  $v$  and  $w$  and their derivatives are disregarded relative to the first powers of these quantities, as a result of which the validity of these formulas is confined to relatively small  $v$  and  $w$ .

The problem now is to so define  $v$  and  $w$  that for given curvature  $\kappa$  of the shell axis the energy of form change  $U$  assumes a minimum value; i.e., to solve the variation problem:

$$U = U_1 + U_2 = \text{Min} \quad (11)$$

## 2. The Orthotropic Circular Cylinder Under Pure Bending

We first analyze the pure bending of the infinitely long orthotropic circular cylinder on the premises of section II, and solve the previously derived variation problem for this particular case. The curvature change  $\Delta \kappa_u$  of the shell section becomes:

$$\Delta \kappa_u = r v''' + \frac{v'}{r} \quad (12)$$

according to equation (10), with  $r$  equal to radius of median shell area. The distance  $h$  of one element of the strained shell from the neutral axis is:

$$h = r \cos t - v \sin t - w \cos t \quad (13)$$

whereby  $w$  is to be replaced according to (9); the significance of  $t$  is seen from figure 12. The variation problem (11), for which the solution could equally well be arrived by integration of the correlated Eulerian differential equation, is solved directly by the formula (Ritz's method):

$$v = r \sum_{j=1}^n A_j \sin 2 j t \quad (14)$$

No terms other than those given can appear in the formula for  $v$  for reasons of symmetry. With (14) and allowance for (12), (13), and (9), equations (6) and (7) give:

$$J_1 = \frac{4\pi}{r} \sum_{j=1}^n j^2 (4 j^2 - 1)^2 A_j^2 \quad (15)$$

$$J_2 = \pi r^3 (1 - 3 A_1) \quad (16)$$

In the determination of  $J_2$  the squares and products of  $v$  and  $w$  are neglected relative to the first powers of these values. The conditions for minimum energy of form change  $U$  are the  $n$  equations:

$$\frac{\partial U}{\partial A_j} = 0 \quad (j = 1, \dots, n)$$

or

$$\frac{\partial J_1}{\partial A_j} = - \frac{12 N}{r^4} \frac{\partial J_2}{\partial A_j} \quad (17)$$

with

$$N = \frac{s_m \kappa^2 r^4 (1 - v^2)}{s^3} \quad (18)$$

With (15) equation (17) becomes:

$$\frac{8\pi}{r} j^2 (4j^2 - 1)^2 A_j = - \frac{12 N}{r^4} \frac{\partial J_2}{\partial A_j}$$

From these equations, the quantities  $A_j$  can be computed:

$$A_1 = \frac{N}{2}, \quad A_j = 0 \quad (j = 2, \dots, n)$$

Hereby  $n$  may be of arbitrary size; that is,

$$v = \frac{N}{2} r \sin 2t$$

is the exact solution of the variation problem (11). The bending moment  $B$  becomes:

$$B = \frac{dU}{d\kappa} = \frac{\partial U}{\partial \kappa} = E s_m \kappa J_2 = \pi E s_m \kappa r^3 \left(1 - \frac{3}{2} N\right) \quad (19)$$

The bending moment reaches its maximum value  $B_{kr}$  if equation

$$\frac{dB}{d\kappa} = \frac{\partial B}{\partial \kappa} + \frac{\partial B}{\partial N} \frac{dN}{d\kappa} = 0 \quad (20)$$

is fulfilled. Equation (20) gives:  $N = \frac{2}{9}$ .

By observing (18), we have:

$$B_{kr} = C \frac{E}{\sqrt{1 - v^2}} r s \sqrt{s s_m} \quad (21)$$

$$C = \frac{2\sqrt{2}\pi}{9} = 0.987$$

Putting

$$B_{kr} = W \sigma_{kr}$$

whereby

$$W = \pi r^2 s_m$$

we find:

$$\sigma_{kr} = c \frac{E}{\sqrt{1 - v^2}} \frac{s}{r} \sqrt{\frac{s}{s_m}} \quad (22)$$

$$c = \frac{2\sqrt{2}}{9} = 0.314$$

but  $\sigma_{kr}$  is only a fictitious stress since  $W$  is the section modulus of the unstrained circular section.

Allowing for the squares and products of  $v$  and  $w$ , disregarded in equation (16), we have:

$$\begin{aligned}
 J_2 &= \pi r^3 (1 - 3A_1) + \oint (v \sin t + w \cos t)^2 ds \\
 &= \pi r^3 \left( 1 - 3A_1 + \frac{5}{2} A_1^2 + \frac{5}{2} A_1 A_2 \right. \\
 &\quad \left. + \frac{17}{2} A_2^2 + \frac{45}{2} A_2 A_3 + \frac{37}{2} A_3^2 + \dots \right) \quad (23)
 \end{aligned}$$

Then the equations (17) read, for  $n = 3$ , for example:

$$\left. \begin{aligned}
 3 A_1 + \left( \frac{5}{2} A_1 + \frac{5}{4} A_2 \right) N &= \frac{3}{2} N \\
 300 A_2 + \left( \frac{5}{4} A_1 + \frac{17}{2} A_2 + \frac{45}{4} A_3 \right) N &= 0 \\
 3675 A_3 + \left( \frac{45}{4} A_2 + \frac{37}{2} A_3 \right) N &= 0
 \end{aligned} \right\} \quad (24)$$

from which  $A_1$  to  $A_3$  (up to  $A_n$  in general) can be obtained. The bending moment

$$B = \frac{dU}{d\kappa} = \frac{\partial U}{\partial \kappa} = E s_m \kappa J_2 \quad (25)$$

reaches a maximum value if

$$\frac{dB}{d\kappa} = \frac{\partial B}{\partial \kappa} + \frac{dN}{d\kappa} \sum_{j=1}^n \frac{\partial B}{\partial A_j} \frac{dA_j}{dN} = 0 \quad (26)$$

This equation gives  $N$  and, by observing (18), (23), and (25), the critical bending moment. It again yields the equations (21) and (22) for  $B_{kr}$  and  $\sigma_{kr}$  but with different coefficients  $C$  and  $c$ . It is:

$$C = 1.22 \quad \text{and} \quad c = 0.388$$

which values are, as stated before, still not completely correct.

On reaching the critical condition (fig. 12) the relative shortening in diameter of the shell section perpendicular to the neutral axis is:

$$\frac{w_0}{r} = N = \frac{2}{9} \quad (27)$$

if the squares and products of  $v$  and  $w$  are neglected

in (7). The relative lengthening of the diameter coincident with the neutral axis is of the same magnitude. If the squares and products of  $v$  and  $w$  in  $J_2$  are considered, then the relative shortening of the diameter perpendicular to the neutral axis amounts to

$$\frac{w_0}{r} = 2 \sum_{j=1}^n j A_j \quad (28)$$

and the relative lengthening of the diameter coincident with the neutral axis

$$- \frac{w_{\pi/2}}{r} = 2 \sum_{j=1}^n (-1)^{j+1} j A_j \quad (29)$$

Here the values  $A_j$  should be determined from (17) and  $N$  from (26). The values  $w_0/r$  and  $-w_{\pi/2}/r$  together with the correlated values of shells with elliptic section are shown in figures 6 and 7.

The actual critical bending stress  $\sigma_{kr}'$  (in contrast to the fictitious bending stress  $\sigma_{kr}$ ) becomes:

$$\sigma_{kr}' = \frac{B_{kr}}{W'}$$

Thereby the critical bending moment is, according to (19):

$$B_{kr} = E s_m \kappa J_2$$

and the section modulus of the deformed shell section (referred to the neutral axis):

$$W' = \frac{J_2 s_m}{r - w_0}$$

Observance of (18) gives:

$$\sigma_{kr}' = c' \frac{E}{\sqrt{1 - \nu^2}} \frac{s}{r} \sqrt{\frac{s}{s_m}}$$

If the squares and products of  $v$  and  $w$  in equation (7) are neglected, it affords with equation (27):

$$c' = (1 - N) \sqrt{N}$$



Allowance for the squares and products of  $v$  and  $w$ , and observance of (28) gives:

$$c' = (1 - 2 \sum_{j=1}^n j A_j) \sqrt{N}$$

The values computed for  $c'$  are plotted in figure 5.

### 3. Pure Bending of the Orthotropic Elliptic Cylinder

In the following we solve the variation problem (11) for a cylindrical shell of elliptic section. The study is confined to the symmetrical cases of bending about the major or minor axis of the shell section. A rectangular system of coordinates in the plane of the shell section makes the  $x$ -axis coincident with the major, and the  $y$ -axis coincident with the minor, cross-sectional axis (fig. 13). Then the equation of the section of the median shell area - expressed in parameters- reads:

$$x = a \sin t$$

$$y = b \cos t$$

where  $a$  is the major, and  $b$  the minor, half axis of the cross-sectional ellipse. Conformable to (6) and (10), we have:

$$J_1 = \oint \left[ \rho v''' + 2\rho' v'' \left( \rho'' + \frac{1}{\rho} \right) v' - v \frac{\rho'}{\rho^2} \right]^2 du \quad (30)$$

whereby

$$du = a (1 - k^2 \sin^2 t)^{1/2} dt, \quad k^2 = \frac{a^2 - b^2}{a^2}$$

$$\rho = \frac{a}{b} (1 - k^2 \sin^2 t)^{3/2} a, \quad \rho' = -\frac{3}{2} \frac{a}{b} k^2 \sin 2t$$

$$\rho'' = -3 \frac{a}{b} k^2 \cos 2t (1 - k^2 \sin^2 t)^{-1/2} \frac{1}{a}$$

If  $h_g$  is the distance of a shell element from the neutral axis in bending about the major cross-sectional axis, and  $h_k$ , the corresponding distance in bending about the minor axis, we have (cf. fig. 13):

$$h_g = b \cos t - w \cos \varphi - v \sin \varphi \quad (31)$$

$$h_k = a \sin t - w \sin \varphi + v \cos \varphi \quad (32)$$

Here  $\varphi$  is the angle of the normal with the minor axis of the ellipse. It is:

$$\sin \varphi = \frac{b}{a} \sin t (1 - k^2 \sin^2 t)^{-1/2}$$

$$\cos \varphi = \cos t (1 - k^2 \sin^2 t)^{-1/2}$$

According to equation (7) the observance of (31) and (32) in bending about the major cross-sectional axis (denoted hereafter by subscript g) gives:

$$J_{2g} = \oint (b^2 \cos^2 t - 2b w \cos t \cos \varphi - 2b v \cos t \sin \varphi) du \quad (33)$$

and by bending about the minor cross-sectional axis (subscript k):

$$J_{2k} = \oint (a^2 \sin^2 t - 2a w \sin t \sin \varphi + 2a v \sin t \cos \varphi) du \quad (34)$$

The squares and products of  $v$  and  $w$  are neglected against the first powers of these values;  $\rho v'$  can be substituted for  $w$  according to (9).

The variation problem (11) can be solved by the Ritz method. The function  $v$  can be approximated by

$$v = a \sum_{j=1}^n A_j \sin 2j t \quad (35)$$

For reasons of symmetry, no terms other than those given can occur in the formula for  $v$ . With formula (35), equation (30) becomes, after several intermediate computations:

$$J_1 = \frac{4}{a(1 - k^2)} \int_0^{\pi/2} \left( \sum_{j=1}^n A_j K_j \right)^2 dt \quad (36)$$

with

$$K_j = \left\{ 2j \cos 2j t [-4j^2 + (\alpha + \beta \sin^2 t + \gamma \sin^4 t) (1 - k^2 \sin^2 t)^{-2}] + \epsilon \sin 2t \sin 2j t (1 - k^2 \sin^2 t)^{-1} [4j^2 + \{ (1 - k^2 \sin^2 t)^{-2} \}] \right\} (1 - k^2 \sin^2 t)^{1/4}$$

where for abbreviation:

$$1 - 3k^2 = \alpha, \quad 4k^2 = \beta, \quad -2k^4 = \gamma$$

$$\frac{3}{2} k^2 = \epsilon, \quad 1 - k^2 = \zeta$$

The term for  $J_1$  given in (36) is valid in bending about the major, as about the minor, axis of the shell section. The evaluation of the integral in (36) by series development being very tedious, the numerical integration is carried out by the Gauss-Lobatto method (reference 8). The integral is approximately replaced by a sum of  $n$  terms. The summands are the values multiplied by certain weights  $g$  of the to-be integrated function at the interval stops and at  $m - 2$  prescribed points of the interval. The thus-obtained approximation is of the order of  $2m - 1$ ; i.e., a parabola of the  $2m - 1$  degree is exactly integrated by this method. Then equation (36) becomes:

$$J_1 = \frac{2\pi}{a(1-k^2)} \sum_{p=1}^m g_p \left( \sum_{j=1}^n A_j K_{jp} \right)^2 \quad (37)$$

The integrals  $J_{2g}$  and  $J_{2k}$ , conformable to equations (33) and (34) can be exactly defined, i.e.:

$$J_{2g} = 2\pi a^3 \left[ (1-k^2)R - \frac{3-k^2}{2} A_1 - \frac{k^2}{2} A_2 \right] \quad (38)$$

$$J_{2k} = 2\pi a^3 \left[ S + \frac{3-2k^2}{2} A_1 + \frac{k^2}{2} A_2 \right] \quad (39)$$

with

$$R = \frac{2}{\pi} \int_0^{\pi/2} (1-k^2 \sin^2 t)^{1/2} \cos^2 t \, dt = \frac{1}{2} - \frac{1}{4} \left( \frac{1}{2} \right)^2 k^2 - \frac{1}{6} \left( \frac{1 \cdot 3}{2 \cdot 4} \right)^2 \frac{k^4}{3} - \frac{1}{8} \left( \frac{1 \cdot 3 \cdot 5}{2 \cdot 4 \cdot 6} \right)^2 \frac{k^6}{5} - \dots$$

$$S = \frac{2}{\pi} \int_0^{\pi/2} (1-k^2 \sin^2 t)^{1/2} \sin^2 t \, dt = \frac{1}{2} - \frac{3}{4} \left( \frac{1}{2} \right)^2 k^2 - \frac{5}{6} \left( \frac{1 \cdot 3}{2 \cdot 4} \right)^2 \frac{k^4}{3} - \frac{7}{8} \left( \frac{1 \cdot 3 \cdot 5}{2 \cdot 4 \cdot 6} \right)^2 \frac{k^6}{5} - \dots$$

With (35) the energy of form change  $U$  becomes a function of the  $n$  variables  $A_j$  ( $j = 1, \dots, n$ ), and so variation problem (11) reduces to a common "extremum"

problem. The accuracy of the method can be raised at will by increasing  $n$ . But, in general, it affords no possibility to assess the errors. The values  $A_j$ , for which  $U$  becomes a minimum by constant  $\kappa$ , follow from the  $n$  linear equations:

$$\frac{\partial U}{\partial A_j} = 0 \quad (j = 1, \dots, n)$$

or

$$\frac{\partial J_1}{\partial A_j} = - \frac{12 N}{a^4} \frac{\partial J_2}{\partial A_j} \quad (40)$$

with

$$N = \frac{s_m \kappa^2 a^4 (1 - v^2)}{s^3} \quad (41)$$

From equation (37) follows:

$$\frac{\partial J_1}{\partial A_j} = \frac{4\pi}{a (1 - k^2)} \sum_{i=1}^n A_i \sum_{p=1}^m g_p (K_j K_i)_p$$

Then the equations (40) with observance of (38) and (39) become, in bending about the major cross-sectional axis:

$$\left. \begin{aligned} \sum_{i=1}^n A_i \sum_{p=1}^m g_p (K_1 K_i)_p &= 3 (1 - k^2) (3 - k^2) N \\ \sum_{i=1}^n A_i \sum_{p=1}^m g_p (K_2 K_i)_p &= 3k^2 (1 - k^2) N \\ \sum_{i=1}^n A_i \sum_{p=1}^m g_p (K_j K_i)_p &= 0 \quad (j = 3, \dots, n) \end{aligned} \right\} \quad (42)$$

and in bending about the minor cross-sectional axis:

$$\left. \begin{aligned} \sum_{i=1}^n A_i \sum_{p=1}^m g_p (K_1 K_i)_p &= -3 (1 - k^2) (3 - 2k^2) N \\ \sum_{i=1}^n A_i \sum_{p=1}^m g_p (K_2 K_i)_p &= -3k^2 (1 - k^2) N \\ \sum_{i=1}^n A_i \sum_{p=1}^m g_p (K_j K_i)_p &= 0 \quad (j = 3, \dots, n) \end{aligned} \right\} \quad (43)$$

Having defined the values  $A_j$  from (42) and (43), the bending moment  $B$  follows from

$$B = \frac{dU}{dk} = \frac{\partial U}{\partial k} = E s_m k J_2 \quad (44)$$

with  $J_2$  as given in (38) and (39). The bending moment  $B$  reaches its highest (critical) value  $B_{kr}$ , if

$$\frac{dB}{dk} = \frac{\partial B}{\partial k} + \frac{dN}{dk} \left( \frac{\partial B}{\partial A_1} \frac{dA_1}{dN} + \frac{\partial B}{\partial A_2} \frac{dA_2}{dN} \right) = 0 \quad (45)$$

From these equations follow:

$$N_g = \frac{2 (1 - k^2) R}{3 \left[ (3 - k^2) \frac{A_1}{N} + k^2 \frac{A_2}{N} \right]}$$

$$N_k = \frac{- 2S}{3 \left[ (3 - 2k^2) \frac{A_1}{N} + k^2 \frac{A_2}{N} \right]}$$

whereby in the expression for  $N_g$  the values  $A_1$  and  $A_2$  are to be taken from (42) and in the term for  $N_k$  from (43).

By observing (38), (39), and (41), equation (44) gives:

$$B_{kr} = C \frac{E}{\sqrt{1 - v^2}} a s \sqrt{s s_m} \quad (46)$$

with

$$C_g = \frac{4}{\pi} \pi (1 - k^2) R \sqrt{\frac{6 (1 - k^2) R}{(3 - k^2) \frac{A_1}{N} + k^2 \frac{A_2}{N}}}$$

$$C_k = \frac{4}{\pi} \pi S \sqrt{\frac{- 6S}{(3 - 2k^2) \frac{A_1}{N} + k^2 \frac{A_2}{N}}}$$

Defining a fictitious critical bending stress  $\sigma_{kr}$  with

$$B_{kr} = W \sigma_{kr}$$

whereby

$$W_g = \frac{\pi}{4} b (b + 3a) s_m, \quad W_k = \frac{\pi}{4} a (a + 3b) s_m$$

are the section moduli of the shell section with respect to the major and minor cross-sectional axes, we find:

$$\sigma_{kr} = c \frac{E}{\sqrt{1 - \nu^2}} \frac{s}{\rho} \sqrt{\frac{s}{s_m}} \quad (47)$$

with

$$c_g = \frac{16}{9} \frac{R}{3 + \sqrt{1 - k^2}} \sqrt{\frac{6 (1 - k^2) R}{(3 - k^2) \frac{A_1}{N} + k^2 \frac{A_2}{N}}}$$

$$c_k = \frac{16}{9} \frac{(1 - k^2) S}{1 + 3\sqrt{1 - k^2}} \sqrt{\frac{-6S}{(3 - 2k^2) \frac{A_1}{N} + k^2 \frac{A_2}{N}}}$$

Figures 14 to 16 show the values  $C_g$  and  $C_k$  and  $\frac{1}{C_k}$  plotted against  $k^2$  and  $n$ . A proof of the convergence of the method is withheld in the present report. Even so, the diagrams manifest the good convergence for small  $k^2$ , while for higher  $k^2$ , it is less good. But even in this range the curves toward which the values  $C_g$  and  $\frac{1}{C_k}$  strive, can be plotted with sufficient accuracy. Figure 4 shows the values  $c_g$  and  $c_k$  plotted against  $k^2$ .

Observance of the squares of products of  $v$  and  $w$ , disregarded in (33) and (34), reveals the right-hand sides of equations (38) and (39) augmented by the terms:

$$\oint (w \cos \varphi + v \sin \varphi)^2 du = \frac{a^3}{1 - k^2} \int_0^{2\pi} \left( \sum_{j=1}^n A_j L_j \right)^2 dt \quad (48)$$

and

$$\oint (w \sin \varphi - v \cos \varphi)^2 du = a^3 \int_0^{2\pi} \left( \sum_{j=1}^n A_j M_j \right)^2 dt \quad (49)$$

Hereby

$$L_j = 2j (1 - k^2 \sin^2 t)^{3/4} \cos t \cos 2j t \\ + (1 - k^2) (1 - k^2 \sin^2 t)^{-1/4} \sin t \sin 2j t$$

$$M_j = 2j (1-k^2 \sin^2 t)^{3/4} \sin t \cos 2j t \\ - (1-k^2 \sin^2 t)^{-1/4} \cos t \sin 2j t$$

Evaluating the integrals in (48) and (49), conformable to Gauss-Lobatto, the equations (38) and (39) are replaced by

$$J_{2g} = 2\pi a^3 \left[ (1-k^2) R - \frac{3-k^2}{2} A_1 - \frac{k^2}{2} A_2 \right. \\ \left. + \frac{1}{1-k^2} \sum_{p=1}^m \varepsilon_p \left( \sum_{j=1}^n A_j L_{jp} \right)^2 \right] \quad (50)$$

$$J_{2k} = 2\pi a^3 \left[ S + \frac{3-2k^2}{2} A_1 + \frac{k^2}{2} A_2 \right. \\ \left. + \sum_{p=1}^m \varepsilon_p \left( \sum_{j=1}^n A_j M_{jp} \right)^2 \right] \quad (51)$$

In bending about the major cross-sectional axis, the equations defining  $A_j$  are:

$$\left. \begin{aligned} & \sum_{i=1}^n A_i \sum_{p=1}^m \varepsilon_p (K_1 K_i)_p \\ & + 12 N \sum_{i=1}^n A_i \sum_{p=1}^m \varepsilon_p (L_1 L_i)_p = 3(1-k^2) (3-k^2) N \\ & \sum_{i=1}^n A_i \sum_{p=1}^m \varepsilon_p (K_2 K_i)_p \\ & + 12 N \sum_{i=1}^n A_i \sum_{p=1}^m \varepsilon_p (L_2 L_i)_p = 3k^2 (1-k^2) N \\ & \sum_{i=1}^n A_i \sum_{p=1}^m \varepsilon_p (K_j K_i)_p \\ & + 12 N \sum_{i=1}^n A_i \sum_{p=1}^m \varepsilon_p (L_j L_i)_p = 0 \quad (j=3, \dots, n) \end{aligned} \right\} \quad (52)$$

and for bending about the minor cross-sectional axis:

$$\begin{aligned}
& \sum_{i=1}^n A_i \sum_{p=1}^m \epsilon_p (K_1 K_i)_p \\
& + 12 (1-k^2) N \sum_{i=1}^n A_i \sum_{p=1}^m \epsilon_p (M_1 M_i)_p \\
& \qquad \qquad \qquad = -3 (1-k^2) (3-2k^2) N \\
& \sum_{i=1}^n A_i \sum_{p=1}^m \epsilon_p (K_2 K_i)_p \\
& + 12 (1-k^2) N \sum_{i=1}^n A_i \sum_{p=1}^m \epsilon_p (M_2 M_i)_p \\
& \qquad \qquad \qquad = -3k^2 (1-k^2) N \\
& \sum_{i=1}^n A_i \sum_{p=1}^m \epsilon_p (K_j K_i)_p \\
& + 12 (1-k^2) N \sum_{i=1}^n A_i \sum_{p=1}^m \epsilon_p (M_j M_i)_p = 0 \\
& \qquad \qquad \qquad (j=3, \dots, n)
\end{aligned} \tag{53}$$

The bending moment  $B$  follows from equation (44), whereby  $J_2$  is given in (50) and (51). The value of  $\kappa$  or  $N$ , for which  $B$  reaches the critical value  $B_{kr}$ , is computed from the equation:

$$\frac{dB}{d\kappa} = \frac{\partial B}{\partial \kappa} + \frac{dN}{d\kappa} \sum_{j=1}^n \frac{\partial B}{\partial A_j} \frac{dA_j}{dN} = 0$$

or

$$\begin{aligned}
& 2 (1-k^2) R - (3-k^2) A_1 - k^2 A_2 + \frac{2}{1-k^2} \sum_{p=1}^m \epsilon_p \left( \sum_{j=1}^n A_j L_{jp} \right)^2 \\
& - 2N \left[ (3-k^2) \frac{dA_1}{dN} + k^2 \frac{dA_2}{dN} \right] \\
& + \frac{8N}{1-k^2} \sum_{i=1}^n \sum_{j=1}^n A_j \sum_{p=1}^m \epsilon_p (L_i L_j)_p \frac{dA_i}{dN} = 0 \tag{54}
\end{aligned}$$

for bending about the major axis and



$$\begin{aligned}
2S + (3-2k^2) A_1 + k^2 A_2 + 2 \sum_{p=1}^m \epsilon_p \left( \sum_{j=1}^n A_j M_{jp} \right)^2 \\
+ 2N \left[ (3-2k^2) \frac{dA_1}{dN} + k^2 \frac{dA_2}{dN} \right] \\
+ 8N \sum_{i=1}^n \sum_{j=1}^n A_j \sum_{p=1}^m \epsilon_p (M_i M_j)_p \frac{dA_i}{dN} = 0 \quad (55)
\end{aligned}$$

for bending about the minor axis of the shell section.

The results for  $B_{kr}$  and  $\sigma_{kr}$  are again the equations (46) and (47) but with different coefficients  $C$  and  $c$ . The thus-obtained values  $c_g$  and  $c_k$  are included in figure 4.

The strain in the originally elliptic section is obtained from the functions  $v$  and  $w$  known after the values  $A_j$  have been determined. Assume that the relative length changes of the half axes of the shell section upon reaching the critical conditions are given (fig. 13). In bending about the major axis of the section, the relative contraction of the minor half axis  $b$  becomes:

$$\frac{w_0}{b} = \frac{2}{1-k^2} \sum_{j=1}^n j A_j \quad (56)$$

and the relative lengthening of the major axis  $a$

$$- \frac{w_{\pi/2}}{a} = 2\sqrt{1-k^2} \sum_{j=1}^n (-1)^{j+1} j A_j \quad (57)$$

In bending about the minor axis of the section the relative shortening of the major half axis  $a$  becomes:

$$\frac{w_{\pi/2}}{a} = -2\sqrt{1-k^2} \sum_{j=1}^n (-1)^{j+1} j A_j \quad (58)$$

and the relative lengthening of the minor half axis  $b$  is:

$$- \frac{w_0}{b} = \frac{-2}{1-k^2} \sum_{j=1}^n j A_j \quad (59)$$

If the squares and products of the displacement components  $v$  and  $w$  are neglected against the first powers of these values, it is necessary to write:

$$N_g = \frac{2 (1 - k^2) R}{3 \left[ (3 - k^2) \frac{A_1}{N} + k^2 \frac{A_2}{N} \right]}$$

$$N_k = \frac{-2S}{3 \left[ (3 - 2k^2) \frac{A_1}{N} + k^2 \frac{A_2}{N} \right]}$$

in the equations (56) to (59), while if these squares and products of  $v$  and  $w$  are allowed for,  $N_g$  and  $N_k$  must be determined from (54) and (55). The numerical values of  $w_0/b$ , etc., are illustrated in figures 6 and 7 for various  $k^2$ .

The actual critical bending stress  $\sigma_{kr}'$  (in contrast to the fictitious stress  $\sigma_{kr}$  referred to the undeformed section), is readily obtainable. In bending about the major axis of the section, it is:

$$\sigma_{gkr}' = \frac{B_{gkr}}{W_g'}$$

Hereby the critical moment is, according to equation (44):

$$B_{gkr} = E s_m \kappa J_{2g}$$

with

$$\kappa = \frac{s}{a^2 \sqrt{1 - v^2}} \sqrt{\frac{s}{s_m} N_g}$$

and the section modulus of the strained shell section (referred to the major axis) becomes:

$$W_g' = \frac{J_{2g} s_m}{b - w_0}$$

With observance of equation (56), we find:

$$\sigma_{gkr}' = c_g' \frac{E}{\sqrt{1 - \nu^2}} \frac{s}{\rho_g} \sqrt{\frac{s}{s_m}}$$

$$c_g' = \left[ 1 - \frac{2}{1 - k^2} \sum_{j=1}^n j A_j \right] \sqrt{N_g}$$

Accordingly, the actual critical bending stress in bending about the minor cross-sectional axis is established at:

$$\sigma_{kkr}' = c_k' \frac{E}{\sqrt{1 - \nu^2}} \frac{s}{\rho_k} \sqrt{\frac{s}{s_m}}$$

$$c_k' = (1 - k^2) \left[ 1 + 2 \sqrt{1 - k^2} \sum_{j=1}^n (-1)^{j+1} j A_j \right] \sqrt{N_k}$$

The values of  $c_g'$  and  $c_k'$  are shown plotted against  $k$  in figure 5.

## REFERENCES

1. Von Kármán, T.: Über die Formänderung dünnwandiger Rohre, insbesondere federnder Ausgleichsrohre. Z.V.D.I., Bd. 55, Heft 45, 1911, S. 1889-1895.
2. Brazier, L. G.: The Flexure of Thin Cylindrical Shells and Other "Thin" Sections. R. & M. No. 1081, British A.R.C., 1927; and Proc. Roy. Soc., London, Ser. A., vol. 116, 1927, pp. 104-114.
3. Pippard, A. J. S.: Note on the Distortion of Thin Tubes Under Flexure. R. & M. No. 1465, British A.R.C., 1932.
4. Chwalla, E.: Reine Biegung schlanker, dünnwandiger Rohre mit gerader Achse. Z.f.a.M.M., Bd. 13, 1933, S. 48-53.
5. Mossman, R. W., and Robinson, R. G.: Bending Tests of Metal Monocoque Fuselage Construction. T.N. No. 357, N.A.C.A., 1930.
6. Lundquist, E. E.: Strength Tests of Thin-Walled Duralumin Cylinders in Pure Bending. T.N. No. 479, N.A.C.A., 1933.
7. Younger, J. E.: Principle of Similitude as Applied to Research on Thin-Sheet Structures. Aeronautical Engineering, vol. V, no. 4, 1933, pp. 163-169.

## VI. APPENDIX

## Results of Previous Studies

a) Theoretical.-- Brazier (reference 2) treats the pure bending of a circular cylinder of infinite length, wherein he neglects the higher powers of the displacement components  $v$  and  $w$  relative to the first powers of these quantities. He arrives at a differential equation which must be exactly solved. Chwalla (reference 4) does not make this omission in his analysis of the work of form change corresponding to the tension stresses. His solution is an approximation evolved on the basis of an elliptic formula for the shape of the strained section of the circular cylinder. Nothing can be said about the magnitude of the errors. Chwalla obtains a somewhat different numerical factor in the formula for the critical bending moment from that given in the present article - probably due to the fact that he does not use as mathematical expression for the assumption of a constant arc length of the shell section the differential equation (9), which is only valid for small  $v$  and  $w$ . He rather defines correlated pairs of diameters of the elliptically deformed section, so that the circumference of the cross section remains constant and equal to the circumference of the median surface of the undeformed shell, regardless of the magnitude of the strain.

The principal results of Brazier and Chwalla have been tabulated in table III.

Brazier likewise approximated the critical bending moments at which local instability phenomena (bulging) are imminent. Because he assumes the whole shell to be as adversely stressed as the extreme fiber in the compression zone, his values for the theoretical critical moment are too low. For this reason, and in consequence of the great influence of preliminary wrinkling through which the moment, at which a perceptible wrinkling actually starts is, under certain circumstances, markedly reduced, the practical value of this analysis is less great. Besides, he uses a formula for the critical stress of an axially compressed cylinder containing the factor  $\frac{k-1}{k+1}$  (Southwell's method), which is now omitted after the works of H. Lorenz and K. v. Sanden (reference 9). Without this factor, the values for the critical bending moment become slightly

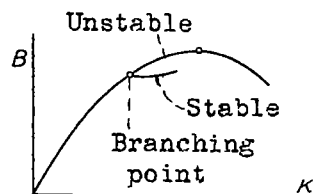
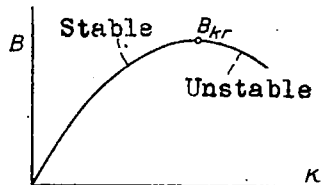
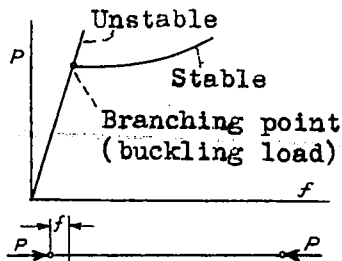
greater. But the noteworthy fact is, that this calculation of the critical bending moment results in a formula of the same construction as Brazier's other consideration.

b) Experimental data.— The available results of tests on circular cylinders in bending are plotted against  $r/s$  and  $l/r$  ( $l$  = length of cylinder) in figures 17 to 19 (references 2, 5, 6, and 7).

TABLE III. Theoretical Results by Brazier and Chwalla

	According to Brazier	According to Chwalla
1. Critical bending moment  (with $\nu=0.3$ )	$B_{kr}=0.987 \frac{E}{\sqrt{1-\nu^2}} r s^2$  $B_{kr}=1.035 E r s^2$	$B_{kr}=1.19 E r s^2$
2. Pertinent curvature of shell axis ( $\nu=0.3$ )	$\kappa=0.494 \frac{s}{r^2}$	$\kappa=0.806 \frac{s}{r^2}$
3. Pertinent relative shortening of diam- eter perpendicular to the neutral axis	$\frac{w_0}{r} = 0.222$	$\frac{w_0}{r} = 0.365$
4. Pertinent relative lengthening of diam- eter coinciding with the neutral axis	$\frac{w_{\pi/2}}{r} = 0.222$	$\frac{w_{\pi/2}}{r} = 0.307$
5. Fictitious critical bending stress ( $\nu=0.3$ )	$\sigma_{kr} = 0.329 E \frac{s}{r}$	$\sigma_{kr} = 0.379 E \frac{s}{r}$
6. Real critical bending stress ( $\nu=0.3$ )	$\sigma_{kr}' = 0.385 E \frac{s}{r}$	$\sigma_{kr}' = 0.523 E \frac{s}{r}$

Translation by J. Vanier,  
National Advisory Committee  
for Aeronautics.



$B \left( \text{---} \text{---} \text{---} \right) B$

Figures 1-3.- Instability phenomena on elastic bodies.

○ values  $c'_g$ ,  $c'_k$  with allowance for the squares and products of  $v$  and  $w$ .

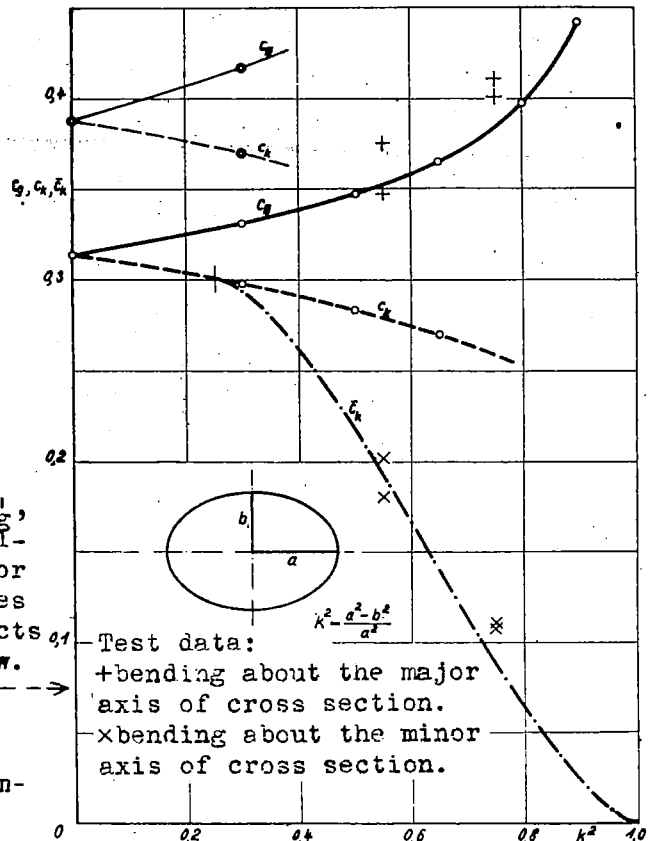
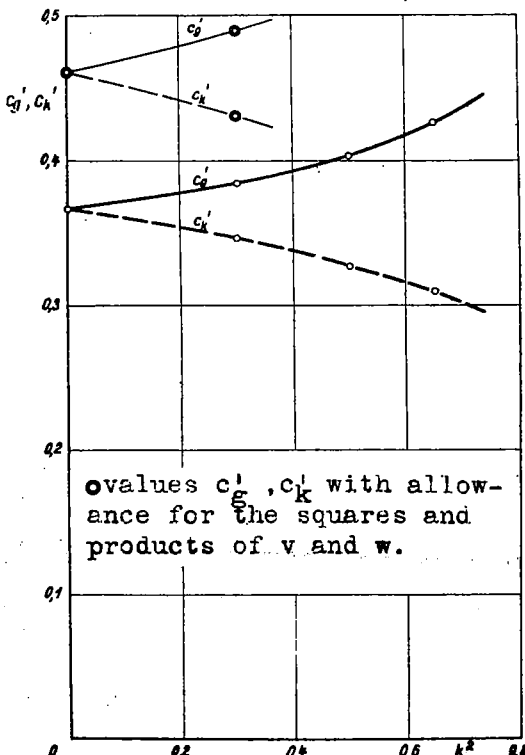
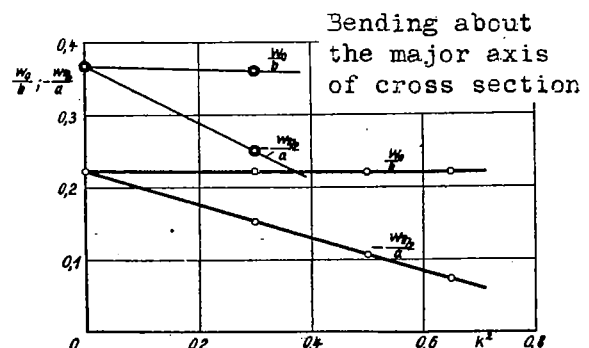


Figure 4.- Values  $c'_g$ ,  $c'_k$ ,  $c_k$  versus  $k^2$ .



○ values  $c'_g$ ,  $c'_k$  with allowance for the squares and products of  $v$  and  $w$ .



○ values  $w_0/b$ ,  $-w_{pi/2}/a$  with allowances for the squares and products of  $v$  and  $w$ .

Figure 6.-  $w_0/b$  and  $-w_{pi/2}/a$  versus  $k^2$ .

Figure 5.- Values  $c'_g$ ,  $c'_k$  versus  $k^2$ .

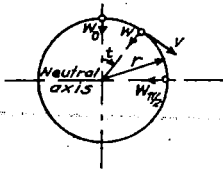


Figure 12.- Section of circular cylinder.

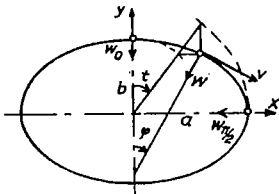


Figure 13.- Section of elliptic cylinder.

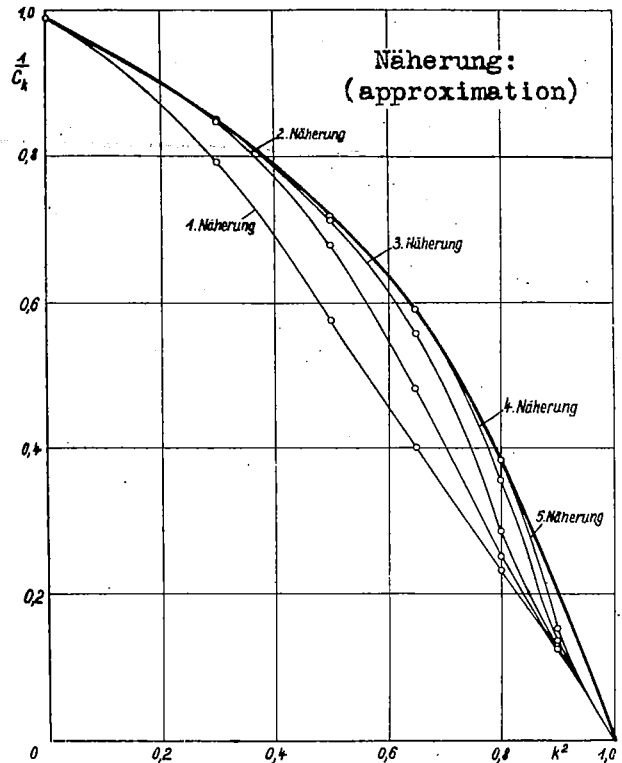


Figure 15.-  $1/C_k$  versus  $k^2$  (bending about minor axis.)

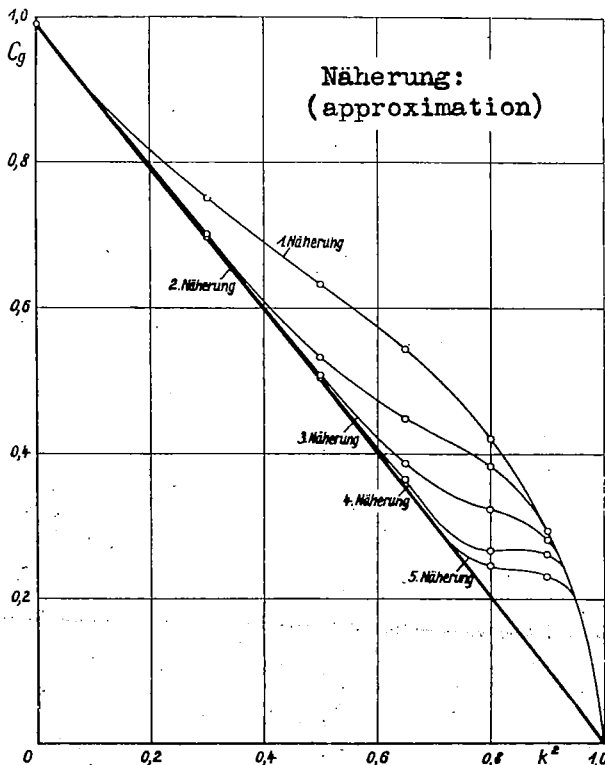


Figure 14.-  $C_g$  versus  $k^2$  (bending about major axis of section.)

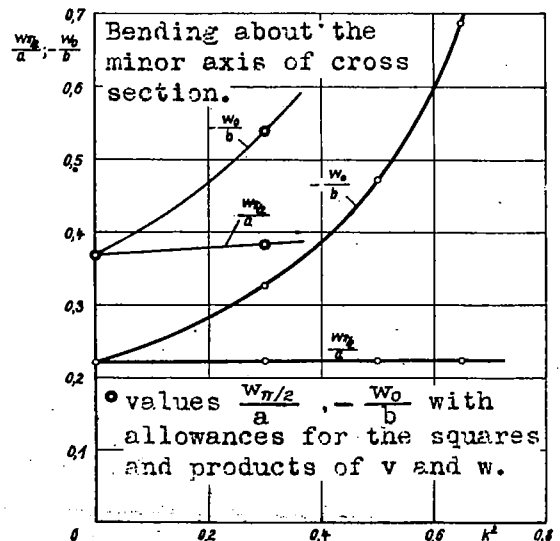


Figure 7.-  $\frac{w_{\pi/2}}{a}$  and  $-w_0/b$  versus  $k^2$



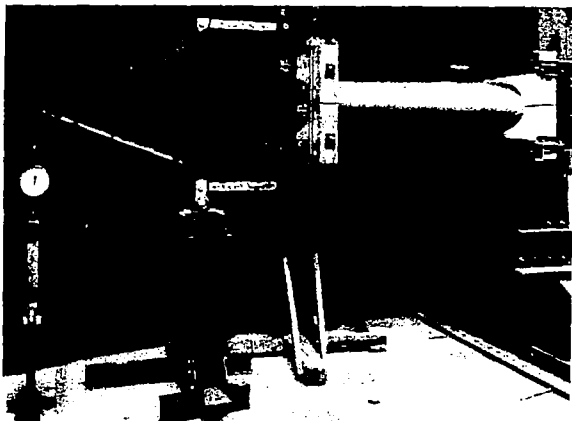


Figure 8.- Loading apparatus.



Figure 9.- Cylinder 1 after failing  
in bending about the major  
axis of the section.

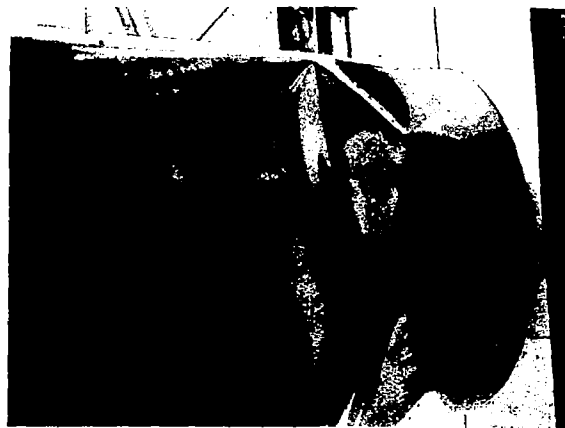


Figure 10.- Cylinder 2 after failing  
in bending about the major  
axis of the section.

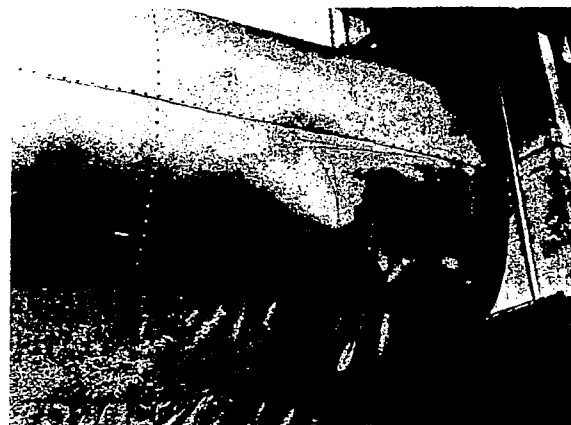


Figure 11.- Cylinder 2 after failing  
in bending about the minor  
axis of the section.

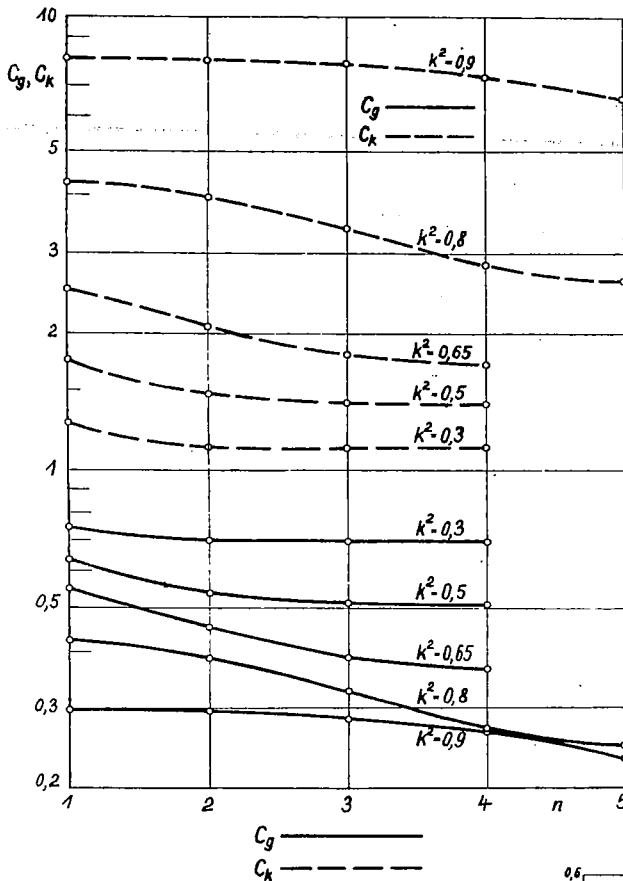


Figure 16.-  $C_g, C_k$  versus  $n$  for different  $k^2$ .

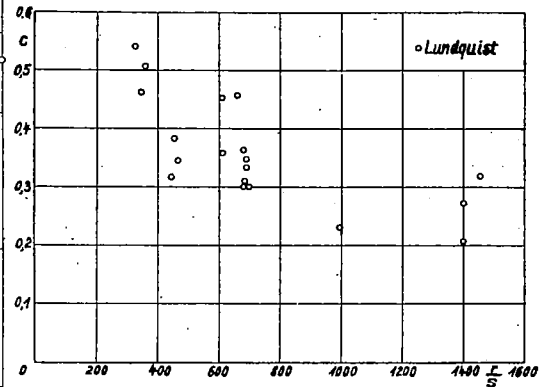


Figure 18.-  $c$  versus  $r/s$  for  $l/r=1.0$  according to tests with isotropic circular cylinders.

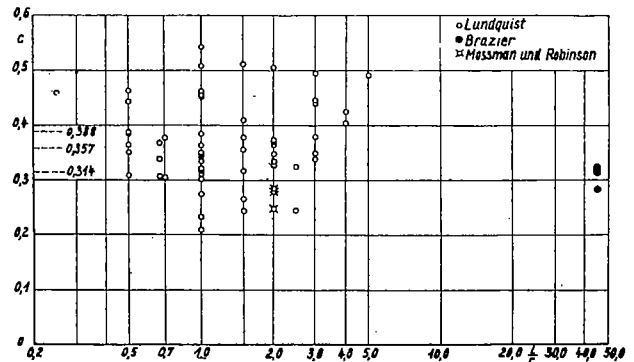


Figure 19.-  $c$  versus  $l/r$  according to tests on isotropic circular cylinders.

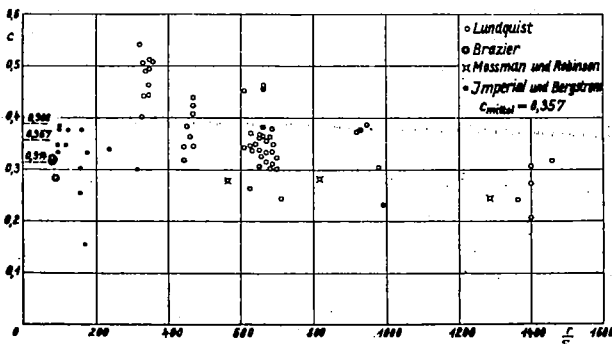


Figure 17.-  $c$  versus  $r/s$  according to tests with isotropic circular cylinders.